Roundoff Noise Minimization for 2-D State-Space Digital Filters Using Joint Optimization of Error Feedback and Realization

Takao Hinamoto, *Fellow, IEEE*, Hiroaki Ohnishi, and Wu-Sheng Lu, *Fellow, IEEE*

***Abstract*—The joint optimization problem of error feedback and realization for two-dimensional (2-D) state-space digital filters to minimize the effects of roundoff noise at the filter output subject to L_2-norm dynamic-range scaling constraints is investigated. It is shown that the problem can be converted into an unconstrained optimization problem by using linear-algebraic techniques. The unconstrained optimization problem at hand is then solved iteratively by applying an efficient quasi-Newton algorithm with closed-form formulas for key gradient evaluation. Analytical details are given as to how the proposed technique can be applied to the cases where the error-feedback matrix is a general, block-diagonal, diagonal, or block-scalar matrix. A case study is presented to illustrate the utility of the proposed technique.**

***Index Terms*—Error feedback, joint optimization, L_2-scaling constraints, roundoff noise minimization, state-space realization, 2-D digital filters.**

I. Introduction

When implementing recursive digital filters in fixed-point arithmetic, the problem of reducing the effects of roundoff noise at the filter output is of critical importance. Error feedback (EF) is a useful tool for the reduction of finite-word-length (FWL) effects in recursive digital filters. Many EF techniques have been reported in the past for one-dimensional (1-D) recursive digital filters [1]–[10], and more recently for two-dimensional (2-D) recursive digital filters [11]–[15]. The roundoff noise can also be reduced by introducing a delta operator to recursive digital filters [16]–[18] or by applying a new structure based on the concept of polynomial operators for digital filter implementation [19]. Another useful approach is to construct the state-space filter structure for the roundoff noise gain to be minimized by applying a linear transformation to state-space coordinates subject to L_2-norm dynamic-range scaling constraints [20]–[23]. The problem of synthesizing such a state-space filter structure with minimum roundoff noise has been explored for 2-D state-space digital filters [24]–[27]. As a natural extension of the aforementioned methods, efforts have been made to develop new methods that combine EF and realization for achieving better performance [28]–[30]. Separately optimized analytical algorithms have been proposed for either 1-D [28] or 2-D [29] state-space digital filters. In [28] and [29], jointly optimized iterative algorithms have also been considered for filters with a general or scalar EF matrix. In [30], a jointly optimized iterative algorithm has been developed for 1-D state-space digital filters with a general, diagonal, or scalar EF matrix by applying a quasi-Newton method.

This paper investigates the problem of jointly optimizing EF and realization for 2-D state-space digital filters to minimize the roundoff noise subject to L_2-norm dynamic-range scaling constraints. To this end, an iterative technique which relies on an efficient quasi-Newton algorithm [31] is developed. It is shown that the constrained optimization problem can be converted into an unconstrained optimization problem by using linear-algebraic techniques. The proposed technique can be applied to the cases where the EF matrix is a general, block-diagonal, diagonal, or block-scalar matrix. A case study is presented to illustrate the algorithm proposed and to demonstrate its performance.

Throughout this paper, $\boldsymbol{I}_n$ stands for the identity matrix of dimension $n \times n$, $\oplus$ and $\cup$ are used to denote the direct sum and the set union of matrices, respectively, the transpose (conjugate transpose) of a matrix $\boldsymbol{A}$ is indicated by $\boldsymbol{A}^T$ ($\boldsymbol{A}^*$), and the trace and ith diagonal element of a square matrix $\boldsymbol{A}$ are denoted by $\mathrm{tr}[\boldsymbol{A}]$ and $(\boldsymbol{A})_{ii}$, respectively.

II. 2-D State-Space Digital Filters With Error Feedback

Suppose that a local state-space (LSS) model $(\boldsymbol{A}, \boldsymbol{b}, \boldsymbol{c}, d)_{m,n}$ for 2-D recursive digital filters is described by [32]

$$\begin{aligned}\boldsymbol{x}_{11}(i,j) &= \boldsymbol{A}\boldsymbol{x}(i,j) + \boldsymbol{b}u(i,j)\\ y(i,j) &= \boldsymbol{c}\boldsymbol{x}(i,j) + du(i,j)\end{aligned} \tag{1}$$

where

$$\boldsymbol{x}_{11}(i,j) = \begin{bmatrix}\boldsymbol{x}^h(i+1,j)\\ \boldsymbol{x}^v(i,j+1)\end{bmatrix}, \quad \boldsymbol{x}(i,j) = \begin{bmatrix}\boldsymbol{x}^h(i,j)\\ \boldsymbol{x}^v(i,j)\end{bmatrix}$$

$$\boldsymbol{A} = \begin{bmatrix}\boldsymbol{A}_1 & \boldsymbol{A}_2\\ \boldsymbol{A}_3 & \boldsymbol{A}_4\end{bmatrix}, \quad \boldsymbol{b} = \begin{bmatrix}\boldsymbol{b}_1\\ \boldsymbol{b}_2\end{bmatrix}, \quad \boldsymbol{c} = [\boldsymbol{c}_1 \quad \boldsymbol{c}_2]$$

with an $m \times 1$ horizontal state vector $\boldsymbol{x}^h(i,j)$, an $n \times 1$ vertical state vector $\boldsymbol{x}^v(i,j)$, a scalar input $u(i,j)$, a scalar output $y(i,j)$, and real constant matrices $\boldsymbol{A}_1$, $\boldsymbol{A}_2$, $\boldsymbol{A}_3$, $\boldsymbol{A}_4$, $\boldsymbol{b}_1$, $\boldsymbol{b}_2$, $\boldsymbol{c}_1$, $\boldsymbol{c}_2$, and d of appropriate dimensions. The LSS model in (1) is assumed to be bounded-input bounded-output (BIBO)

Manuscript received July 7, 2005; accepted January 4, 2006. The associate editor coordinating the review of this manuscript and approving it for publication was Prof. Brian L. Evans.

T. Hinamoto and H. Ohnishi are with the Graduate School of Engineering, Hiroshima University, Hiroshima, Japan (e-mail: hinamoto@hiroshima-u.ac.jp).

W.-S. Lu is with the Department of Electrical and Computer Engineering, University of Victoria, Victoria, B.C. V8W 3P6, Canada (e-mail: wslu@ece.uvic.ca).

Digital Object Identifier 10.1109/TSP.2006.881178

stable, separately locally controllable, and separately locally observable [33].

Due to finite register sizes, we impose FWL constraints on the local state vector $\boldsymbol{x}(i,j)$, the input, the output, and the coefficients in the realization $(\boldsymbol{A},\boldsymbol{b},\boldsymbol{c},d)_{m,n}$. Assuming that the quantization is performed before matrix-vector multiplication, the actual FWL filter of (1) is implemented as

$$\begin{aligned}\tilde{\boldsymbol{x}}_{11}(i,j) &= \boldsymbol{A}\boldsymbol{Q}[\tilde{\boldsymbol{x}}(i,j)] + \boldsymbol{b}u(i,j)\\ \tilde{y}(i,j) &= \boldsymbol{c}\boldsymbol{Q}[\tilde{\boldsymbol{x}}(i,j)] + du(i,j)\end{aligned} \tag{2}$$

where each component of matrices $\boldsymbol{A},\boldsymbol{b},\boldsymbol{c}$, and d assumes an exact fractional B_c-bit representation. The FWL local state vector $\tilde{\boldsymbol{x}}(i,j)$ and the output $\tilde{y}(i,j)$ all have a B-bit fractional representation, while the input $u(i,j)$ is a $(B-B_c)$-bit fraction.

The quantizer $\boldsymbol{Q}[\cdot]$ in (2) rounds the B-bit fraction $\tilde{\boldsymbol{x}}(i,j)$ to $(B-B_c)$ bits after multiplications and additions, where the sign bit is not counted. In a fixed-point implementation, the quantization is usually carried out by two's-complement truncation, which discards the lower bits of a double-precision accumulator. Thus, the quantization error

$$\boldsymbol{e}(i,j) = \tilde{\boldsymbol{x}}(i,j) - \boldsymbol{Q}[\tilde{\boldsymbol{x}}(i,j)] \tag{3}$$

coincides with the residue left in the lower part of $\tilde{\boldsymbol{x}}(i,j)$. The quantization error $\boldsymbol{e}(i,j)$ is modeled as a zero-mean white noise of covariance $\sigma^2\boldsymbol{I}_{m+n}$ with

$$\sigma^2 = \frac{1}{12}2^{-2(B-B_c)}.$$

In order to reduce the filter's roundoff noise, the quantization error $\boldsymbol{e}(i,j)$ is fed back to each input of delay operators through an $(m+n)\times(m+n)$ constant matrix $\boldsymbol{D}$. Under these circumstances, the filter model can be represented as

$$\begin{aligned}\tilde{\boldsymbol{x}}_{11}(i,j) &= \boldsymbol{A}\boldsymbol{Q}[\tilde{\boldsymbol{x}}(i,j)] + \boldsymbol{b}u(i,j) + \boldsymbol{D}\boldsymbol{e}(i,j)\\ \tilde{y}(i,j) &= \boldsymbol{c}\boldsymbol{Q}[\tilde{\boldsymbol{x}}(i,j)] + du(i,j)\end{aligned} \tag{4}$$

where $\boldsymbol{D}$ is referred to as the EF matrix. Subtracting (4) from (1) yields

$$\begin{aligned}\Delta\boldsymbol{x}_{11}(i,j) &= \boldsymbol{A}\Delta\boldsymbol{x}(i,j) + (\boldsymbol{A}-\boldsymbol{D})\boldsymbol{e}(i,j)\\ \Delta y(i,j) &= \boldsymbol{c}\Delta\boldsymbol{x}(i,j) + \boldsymbol{c}\boldsymbol{e}(i,j)\end{aligned} \tag{5}$$

where

$$\begin{aligned}\Delta\boldsymbol{x}(i,j) &= \boldsymbol{x}(i,j) - \tilde{\boldsymbol{x}}(i,j)\\ \Delta\boldsymbol{x}_{11}(i,j) &= \boldsymbol{x}_{11}(i,j) - \tilde{\boldsymbol{x}}_{11}(i,j)\\ \Delta y(i,j) &= y(i,j) - \tilde{y}(i,j).\end{aligned}$$

From (5), it follows that the 2-D transfer function from the quantization error $\boldsymbol{e}(i,j)$ to the filter output $\Delta y(i,j)$ is given by

$$\boldsymbol{G}_D(z_1,z_2) = \boldsymbol{c}(\boldsymbol{Z}-\boldsymbol{A})^{-1}(\boldsymbol{A}-\boldsymbol{D}) + \boldsymbol{c} \tag{6}$$

where $\boldsymbol{Z} = z_1\boldsymbol{I}_m \oplus z_2\boldsymbol{I}_n$.

For the 2-D filter in (4) with EF, the noise gain $I(\boldsymbol{D}) = \sigma_{out}^2/\sigma^2$ is evaluated by

$$I(\boldsymbol{D}) = \mathrm{tr}[\boldsymbol{W}_D] \tag{7}$$

where σ_{out}^2 denotes noise variance at the filter output and

$$\boldsymbol{W}_D = \frac{1}{(2\pi j)^2}\oint_{\Gamma_1}\oint_{\Gamma_2}\boldsymbol{G}_D^*(z_1,z_2)\boldsymbol{G}_D(z_1,z_2)\frac{dz_1dz_2}{z_1z_2}$$

with $\Gamma_i = \{z_i : |z_i| = 1\}$ for $i = 1,2$. Utilizing the 2-D Cauchy integral theorem, we can express matrix $\boldsymbol{W}_D$ in (7) in closed form as

$$\boldsymbol{W}_D = (\boldsymbol{A}-\boldsymbol{D})^T\boldsymbol{W}_o(\boldsymbol{A}-\boldsymbol{D}) + \boldsymbol{c}^T\boldsymbol{c} \tag{8}$$

where matrix $\boldsymbol{W}_o$ is the local observability Gramian defined by

$$\begin{aligned}\boldsymbol{W}_o &= \frac{1}{(2\pi j)^2}\oint_{\Gamma_1}\oint_{\Gamma_2}(\boldsymbol{Z}^*-\boldsymbol{A}^T)^{-1}\boldsymbol{c}^T\boldsymbol{c}(\boldsymbol{Z}-\boldsymbol{A})^{-1}\frac{dz_1dz_2}{z_1z_2}\\ &= \sum_{i=0}^{\infty}\sum_{j=0}^{\infty}\boldsymbol{g}(i,j)^T\boldsymbol{g}(i,j)\end{aligned} \tag{9}$$

with

$$\begin{aligned}\boldsymbol{g}(i,j) &= \boldsymbol{c}\boldsymbol{A}^{(i-1,j)}\begin{bmatrix}\boldsymbol{I}_m & \boldsymbol{0}\\ \boldsymbol{0} & \boldsymbol{0}\end{bmatrix} + \boldsymbol{c}\boldsymbol{A}^{(i,j-1)}\begin{bmatrix}\boldsymbol{0} & \boldsymbol{0}\\ \boldsymbol{0} & \boldsymbol{I}_n\end{bmatrix}\\ \boldsymbol{A}^{(1,0)} &= \begin{bmatrix}\boldsymbol{I}_m & \boldsymbol{0}\\ \boldsymbol{0} & \boldsymbol{0}\end{bmatrix}\boldsymbol{A},\quad \boldsymbol{A}^{(0,1)} = \begin{bmatrix}\boldsymbol{0} & \boldsymbol{0}\\ \boldsymbol{0} & \boldsymbol{I}_n\end{bmatrix}\boldsymbol{A}\\ \boldsymbol{A}^{(0,0)} &= \boldsymbol{I}_{m+n},\quad \boldsymbol{A}^{(-i,j)} = \boldsymbol{0}\ (i\ge 1),\quad \boldsymbol{A}^{(i,-j)} = \boldsymbol{0}\ (j\ge 1)\\ \boldsymbol{A}^{(i,j)} &= \boldsymbol{A}^{(1,0)}\boldsymbol{A}^{(i-1,j)} + \boldsymbol{A}^{(0,1)}\boldsymbol{A}^{(i,j-1)}\\ &= \boldsymbol{A}^{(i-1,j)}\boldsymbol{A}^{(1,0)} + \boldsymbol{A}^{(i,j-1)}\boldsymbol{A}^{(0,1)},\quad (i,j) > (0,0)\end{aligned} \tag{10}$$

and the partial ordering for integer pairs (i,j) used in [32, p. 2].

We remark that matrix $\boldsymbol{W}_o$ in (9) is referred to as the *unit noise matrix* for the 2-D filter in (2) and matrix $\boldsymbol{W}_D$ in (8) is viewed as the *unit noise matrix* for the 2-D filter in (4) with EF specified by the matrix $\boldsymbol{D}$.

In the case where there is no EF in the 2-D filter, the noise gain $I(\boldsymbol{D})$ with $\boldsymbol{D} = \boldsymbol{0}$ can be expressed as

$$I(\boldsymbol{0}) = \mathrm{tr}[\boldsymbol{A}^T\boldsymbol{W}_o\boldsymbol{A} + \boldsymbol{c}^T\boldsymbol{c}] = \mathrm{tr}[\boldsymbol{W}_o]. \tag{11}$$

It is noted that the L_2-norm dynamic-range scaling constraints on the local state vector $\boldsymbol{x}(i,j)$ involve the local controllability Gramian defined by

$$\begin{aligned}\boldsymbol{K}_c &= \frac{1}{(2\pi j)^2}\oint_{\Gamma_1}\oint_{\Gamma_2}(\boldsymbol{Z}-\boldsymbol{A})^{-1}\boldsymbol{b}\boldsymbol{b}^T(\boldsymbol{Z}^*-\boldsymbol{A}^T)^{-1}\frac{dz_1dz_2}{z_1z_2}\\ &= \sum_{i=0}^{\infty}\sum_{j=0}^{\infty}\boldsymbol{f}(i,j)\boldsymbol{f}(i,j)^T\end{aligned} \tag{12}$$

where

$$\boldsymbol{f}(i,j) = \boldsymbol{A}^{(i-1,j)}\begin{bmatrix}\boldsymbol{b}_1\\ \boldsymbol{0}\end{bmatrix} + \boldsymbol{A}^{(i,j-1)}\begin{bmatrix}\boldsymbol{0}\\ \boldsymbol{b}_2\end{bmatrix}.$$

III. Joint Error-Feedback and Realization Optimization

A. Probem Statement

The change of coordinates from local state vector $\boldsymbol{x}(i,j)$ to $\overline{\boldsymbol{x}}(i,j)$, defined by a linear transformation $\overline{\boldsymbol{x}}(i,j) = \boldsymbol{T}^{-1}\boldsymbol{x}(i,j)$ with $\boldsymbol{T} = \boldsymbol{T}_1 \oplus \boldsymbol{T}_4$, transforms the LSS model $(\boldsymbol{A},\boldsymbol{b},\boldsymbol{c},d)_{m,n}$ in (1) to a new realization $(\overline{\boldsymbol{A}},\overline{\boldsymbol{b}},\overline{\boldsymbol{c}},d)_{m,n}$ with

$$\overline{\boldsymbol{A}} = \boldsymbol{T}^{-1}\boldsymbol{A}\boldsymbol{T}, \quad \overline{\boldsymbol{b}} = \boldsymbol{T}^{-1}\boldsymbol{b}, \quad \overline{\boldsymbol{c}} = \boldsymbol{c}\boldsymbol{T}. \tag{13}$$

The local controllability Gramian $\overline{\boldsymbol{K}}_c$ and the local observability Gramian $\overline{\boldsymbol{W}}_o$ in the new realization then satisfy the relations

$$\overline{\boldsymbol{K}}_c = \boldsymbol{T}^{-1}\boldsymbol{K}_c\boldsymbol{T}^{-T}, \quad \overline{\boldsymbol{W}}_o = \boldsymbol{T}^T\boldsymbol{W}_o\boldsymbol{T}. \tag{14}$$

If the L_2-norm dynamic-range scaling constraints specified by

$$(\overline{\boldsymbol{K}}_c)_{ii} = (\boldsymbol{T}^{-1}\boldsymbol{K}_c\boldsymbol{T}^{-T})_{ii} = 1, \quad i = 1,2,\ldots,m+n \tag{15}$$

are imposed on the new realization, then it is known that [25], [26]

$$\min_{\boldsymbol{T}} \operatorname{tr}[\overline{\boldsymbol{W}}_o] = \frac{1}{m}\left(\sum_{i=1}^{m}\sigma_{1i}\right)^2 + \frac{1}{n}\left(\sum_{i=1}^{n}\sigma_{4i}\right)^2 \tag{16}$$

where σ_{1i}^2 for $i = 1,2,\ldots,m$ and σ_{4i}^2 for $i = 1,2,\ldots,n$ are the eigenvalues of the $m \times m$ matrix $\boldsymbol{K}_{1c}\boldsymbol{W}_{1o}$ and the $n \times n$ matrix $\boldsymbol{K}_{4c}\boldsymbol{W}_{4o}$, respectively, and

$$\boldsymbol{K}_c = \begin{bmatrix} \boldsymbol{K}_{1c} & \boldsymbol{K}_{2c} \\ \boldsymbol{K}_{3c} & \boldsymbol{K}_{4c} \end{bmatrix}, \quad \boldsymbol{W}_o = \begin{bmatrix} \boldsymbol{W}_{1o} & \boldsymbol{W}_{2o} \\ \boldsymbol{W}_{3o} & \boldsymbol{W}_{4o} \end{bmatrix}.$$

The LSS model $(\overline{\boldsymbol{A}},\overline{\boldsymbol{b}},\overline{\boldsymbol{c}},d)_{m,n}$ satisfying (15) and (16) simultaneously is known as the *optimal realization* (which is sometimes also referred to as the *optimal filter structure*). A method for synthesizing such a filter structure was proposed in [25] and [26].

If a coordinate transformation $\overline{\boldsymbol{x}}(i,j) = \boldsymbol{T}^{-1}\boldsymbol{x}(i,j)$ with $\boldsymbol{T} = \boldsymbol{T}_1 \oplus \boldsymbol{T}_4$ is applied to the LSS model in (1), then the 2-D filter in (4) with EF can be characterized by

$$\begin{aligned} \tilde{\overline{\boldsymbol{x}}}_{11}(i,j) &= \overline{\boldsymbol{A}}\boldsymbol{Q}[\tilde{\overline{\boldsymbol{x}}}(i,j)] + \overline{\boldsymbol{b}}u(i,j) + \boldsymbol{D}\boldsymbol{e}(i,j) \\ \tilde{y}(i,j) &= \overline{\boldsymbol{c}}\boldsymbol{Q}[\tilde{\overline{\boldsymbol{x}}}(i,j)] + du(i,j). \end{aligned} \tag{17}$$

In this case, the noise gain $I(\boldsymbol{D},\boldsymbol{T})$ can be expressed as a function of matrices $\boldsymbol{D}$ and $\boldsymbol{T} = \boldsymbol{T}_1 \oplus \boldsymbol{T}_4$ in the form

$$I(\boldsymbol{D},\boldsymbol{T}) = \operatorname{tr}[\overline{\boldsymbol{W}}_D] \tag{18}$$

where

$$\overline{\boldsymbol{W}}_D = (\overline{\boldsymbol{A}} - \boldsymbol{D})^T\overline{\boldsymbol{W}}_o(\overline{\boldsymbol{A}} - \boldsymbol{D}) + \overline{\boldsymbol{c}}^T\overline{\boldsymbol{c}}.$$

The roundoff noise minimization problem can now be formulated as follows: given $\boldsymbol{A}$, $\boldsymbol{b}$ and $\boldsymbol{c}$ (and hence $\boldsymbol{W}_o$ and $\boldsymbol{K}_c$), obtain matrices $\boldsymbol{D}$ and $\boldsymbol{T} = \boldsymbol{T}_1 \oplus \boldsymbol{T}_4$ which jointly minimize the noise gain in (18) subject to the scaling constraints in (15).

B. Problem Relaxation and Conversion

In order to reduce solution sensitivity, the objective function in (18) is modified to

$$J(\boldsymbol{D},\boldsymbol{T}) = \operatorname{tr}[(1-\mu)\overline{\boldsymbol{W}}_D + \mu\overline{\boldsymbol{W}}_o] \tag{19}$$

where $0 \le \mu \le 1$ is a scalar parameter that weights the importance of reducing $\operatorname{tr}[\overline{\boldsymbol{W}}_o]$ relative to reducing $\operatorname{tr}[\overline{\boldsymbol{W}}_D]$. Defining

$$\begin{aligned} \hat{\boldsymbol{T}} &= \hat{\boldsymbol{T}}_1 \oplus \hat{\boldsymbol{T}}_4 \\ &= (\boldsymbol{T}_1 \oplus \boldsymbol{T}_4)^T(\boldsymbol{K}_{1c} \oplus \boldsymbol{K}_{4c})^{-1/2} \end{aligned} \tag{20}$$

it follows that

$$\overline{\boldsymbol{K}}_c = \hat{\boldsymbol{T}}^{-T}\begin{bmatrix} \boldsymbol{I}_m & \boldsymbol{K}_{1c}^{-1/2}\boldsymbol{K}_{2c}\boldsymbol{K}_{4c}^{-1/2} \\ \boldsymbol{K}_{4c}^{-1/2}\boldsymbol{K}_{3c}\boldsymbol{K}_{1c}^{-1/2} & \boldsymbol{I}_n \end{bmatrix}\hat{\boldsymbol{T}}^{-1}. \tag{21}$$

This enables one to reduce the scaling constraints in (15) to

$$\begin{aligned} (\hat{\boldsymbol{T}}_1^{-T}\hat{\boldsymbol{T}}_1^{-1})_{ii} &= 1, \quad i = 1,2,\ldots,m \\ (\hat{\boldsymbol{T}}_4^{-T}\hat{\boldsymbol{T}}_4^{-1})_{kk} &= 1, \quad k = 1,2,\ldots,n. \end{aligned} \tag{22}$$

The constraints in (22) simply state that each column in matrices $\hat{\boldsymbol{T}}_1^{-1}$ and $\hat{\boldsymbol{T}}_4^{-1}$ must be a unity vector. It can be verified that these constraints are satisfied if $\hat{\boldsymbol{T}}_1^{-1}$ and $\hat{\boldsymbol{T}}_4^{-1}$ assume the forms

$$\begin{aligned} \hat{\boldsymbol{T}}_1^{-1} &= \left[\frac{\boldsymbol{t}_{11}}{||\boldsymbol{t}_{11}||}, \frac{\boldsymbol{t}_{12}}{||\boldsymbol{t}_{12}||}, \ldots, \frac{\boldsymbol{t}_{1m}}{||\boldsymbol{t}_{1m}||}\right] \\ \hat{\boldsymbol{T}}_4^{-1} &= \left[\frac{\boldsymbol{t}_{41}}{||\boldsymbol{t}_{41}||}, \frac{\boldsymbol{t}_{42}}{||\boldsymbol{t}_{42}||}, \ldots, \frac{\boldsymbol{t}_{4n}}{||\boldsymbol{t}_{4n}||}\right] \end{aligned} \tag{23}$$

where $\boldsymbol{t}_{1i}$ for $i = 1,2,\ldots,m$ and $\boldsymbol{t}_{4j}$ for $j = 1,2,\ldots,n$ are $m \times 1$ and $n \times 1$ real vectors, respectively. In such a case, matrix $\overline{\boldsymbol{W}}_D$ in (18) can be written as

$$\overline{\boldsymbol{W}}_D = \hat{\boldsymbol{T}}[(\hat{\boldsymbol{A}} - \hat{\boldsymbol{T}}^T\boldsymbol{D}\hat{\boldsymbol{T}}^{-T})^T\hat{\boldsymbol{W}}_o(\hat{\boldsymbol{A}} - \hat{\boldsymbol{T}}^T\boldsymbol{D}\hat{\boldsymbol{T}}^{-T}) + \hat{\boldsymbol{C}}]\hat{\boldsymbol{T}}^T \tag{24}$$

where $\hat{\boldsymbol{T}} = \hat{\boldsymbol{T}}_1 \oplus \hat{\boldsymbol{T}}_4$ and

$$\begin{aligned} \hat{\boldsymbol{A}} &= (\boldsymbol{K}_{1c} \oplus \boldsymbol{K}_{4c})^{-1/2}\boldsymbol{A}(\boldsymbol{K}_{1c} \oplus \boldsymbol{K}_{4c})^{1/2} \\ \hat{\boldsymbol{C}} &= (\boldsymbol{K}_{1c} \oplus \boldsymbol{K}_{4c})^{1/2}\boldsymbol{c}^T\boldsymbol{c}(\boldsymbol{K}_{1c} \oplus \boldsymbol{K}_{4c})^{1/2} \\ \hat{\boldsymbol{W}}_o &= (\boldsymbol{K}_{1c} \oplus \boldsymbol{K}_{4c})^{1/2}\boldsymbol{W}_o(\boldsymbol{K}_{1c} \oplus \boldsymbol{K}_{4c})^{1/2}. \end{aligned}$$

Under these circumstances, the objective function in (19) becomes

$$\begin{aligned} J(\boldsymbol{D},\hat{\boldsymbol{T}}) = {} & (1-\mu)\operatorname{tr}[(\hat{\boldsymbol{T}}\hat{\boldsymbol{A}}^T - \boldsymbol{D}^T\hat{\boldsymbol{T}})\hat{\boldsymbol{W}}_o(\hat{\boldsymbol{A}}\hat{\boldsymbol{T}}^T - \hat{\boldsymbol{T}}^T\boldsymbol{D})] \\ & + (1-\mu)\operatorname{tr}[\hat{\boldsymbol{T}}\hat{\boldsymbol{C}}\hat{\boldsymbol{T}}^T] + \mu\operatorname{tr}[\hat{\boldsymbol{T}}\hat{\boldsymbol{W}}_o\hat{\boldsymbol{T}}^T]. \end{aligned} \tag{25}$$

From the foregoing arguments, the problem of obtaining matrices $\boldsymbol{D}$ and $\boldsymbol{T} = \boldsymbol{T}_1 \oplus \boldsymbol{T}_4$ that minimize (19) subject to the scaling constraints in (15) is now converted into an unconstrained optimization problem of obtaining matrices $\boldsymbol{D}$ and $\hat{\boldsymbol{T}} = \hat{\boldsymbol{T}}_1 \oplus \hat{\boldsymbol{T}}_4$ that jointly minimize the noise gain in (25).

C. Optimization Method

Let $\boldsymbol{x}$ be the column vector that collects the variables in matrices $\boldsymbol{D}$, $[\boldsymbol{t}_{11}, \boldsymbol{t}_{12}, \ldots, \boldsymbol{t}_{1m}]$, and $[\boldsymbol{t}_{41}, \boldsymbol{t}_{42}, \ldots, \boldsymbol{t}_{4n}]$. Then, $J(\boldsymbol{D}, \hat{\boldsymbol{T}})$ is a function of $\boldsymbol{x}$, denoted by $J(\boldsymbol{x})$. The proposed algorithm starts with an initial point $\boldsymbol{x}_0$ obtained from an initial assignment $\boldsymbol{D} = \hat{\boldsymbol{T}} = \boldsymbol{I}_{m+n}$. In the kth iteration, a quasi-Newton algorithm updates the most recent point $\boldsymbol{x}_k$ to point $\boldsymbol{x}_{k+1}$ as [31]

$$\boldsymbol{x}_{k+1} = \boldsymbol{x}_k + \alpha_k \boldsymbol{d}_k \tag{26}$$

where

$$\begin{aligned}
\boldsymbol{d}_k &= -\boldsymbol{S}_k \nabla J(\boldsymbol{x}_k) \\
\alpha_k &= \arg\left[\min_{\alpha} \; J(\boldsymbol{x}_k + \alpha \boldsymbol{d}_k)\right] \\
\boldsymbol{S}_{k+1} &= \boldsymbol{S}_k + \left(1 + \frac{\boldsymbol{\gamma}_k^T \boldsymbol{S}_k \boldsymbol{\gamma}_k}{\boldsymbol{\gamma}_k^T \boldsymbol{\delta}_k}\right) \frac{\boldsymbol{\delta}_k \boldsymbol{\delta}_k^T}{\boldsymbol{\gamma}_k^T \boldsymbol{\delta}_k} - \frac{\boldsymbol{\delta}_k \boldsymbol{\gamma}_k^T \boldsymbol{S}_k + \boldsymbol{S}_k \boldsymbol{\gamma}_k \boldsymbol{\delta}_k^T}{\boldsymbol{\gamma}_k^T \boldsymbol{\delta}_k} \\
\boldsymbol{S}_0 &= \boldsymbol{I}, \quad \boldsymbol{\delta}_k = \boldsymbol{x}_{k+1} - \boldsymbol{x}_k, \quad \boldsymbol{\gamma}_k = \nabla J(\boldsymbol{x}_{k+1}) - \nabla J(\boldsymbol{x}_k).
\end{aligned}$$

Here, $\nabla J(\boldsymbol{x})$ is the gradient of $J(\boldsymbol{x})$ with respect to $\boldsymbol{x}$, and $\boldsymbol{S}_k$ is a positive-definite approximation of the inverse Hessian matrix of $J(\boldsymbol{x})$. This iteration process continues until

$$|J(\boldsymbol{x}_{k+1}) - J(\boldsymbol{x}_k)| < \varepsilon \tag{27}$$

where $\varepsilon > 0$ is a prescribed tolerance. If the iteration is terminated at step k, then $\boldsymbol{x}_k$ is deemed as a solution point.

The implementation of (26) requires the gradient of $J(\boldsymbol{x})$. Now we consider the cases where EF matrix is a general, block-diagonal, diagonal, or block-scalar matrix. It is noted that a general EF matrix is often too costly because it requires as many as $(m+n)^2$ explicit multiplications. The cost can be reduced, e.g., by constraining EF matrix to be a block-diagonal or diagonal (block-scalar), which reduces the number of distinct coefficients to $m^2 + n^2$ or $m + n$.

A key quantity for the implementation of the quasi-Newton algorithm is the gradient $\nabla J(\boldsymbol{x})$. In what follows, we derive closed-form expressions of $\nabla J(\boldsymbol{x})$ for the cases where $\boldsymbol{D}$ assumes the form of a general, block-diagonal, diagonal, or block-scalar matrix.

1) Case 1: $\boldsymbol{D}$ Is a General Matrix: From (25), it is evident that the optimal choice of $\boldsymbol{D}$ is given by

$$\boldsymbol{D} = \hat{\boldsymbol{T}}^{-T} \hat{\boldsymbol{A}} \hat{\boldsymbol{T}}^T \tag{28}$$

which leads to

$$J(\hat{\boldsymbol{T}}^{-T} \hat{\boldsymbol{A}} \hat{\boldsymbol{T}}^T, \hat{\boldsymbol{T}}) = \operatorname{tr}[\hat{\boldsymbol{T}} \{(1-\mu)\hat{\boldsymbol{C}} + \mu \hat{\boldsymbol{W}}_o\} \hat{\boldsymbol{T}}^T]. \tag{29}$$

In this case, the number of elements in vector $\boldsymbol{x}$ consisting of $\hat{\boldsymbol{T}} = \hat{\boldsymbol{T}}_1 \oplus \hat{\boldsymbol{T}}_4$ is equal to $m^2 + n^2$, and the gradient of $J(\boldsymbol{x})$ is found to be

$$\begin{aligned}
\frac{\partial J(\boldsymbol{x})}{\partial t_{ij}} &= \lim_{\Delta \to 0} \frac{J(\hat{\boldsymbol{T}}_{ij}) - J(\hat{\boldsymbol{T}})}{\Delta} \\
&= 2\boldsymbol{e}_j^T \hat{\boldsymbol{T}} [(1-\mu)\hat{\boldsymbol{C}} + \mu \hat{\boldsymbol{W}}_o] \hat{\boldsymbol{T}}^T \hat{\boldsymbol{T}} \boldsymbol{g}_{ij}
\end{aligned} \tag{30}$$

where $\hat{\boldsymbol{T}}_{ij}$ is the matrix obtained from $\hat{\boldsymbol{T}}$ with a perturbed (i,j)th component, which is given by [34, p. 655]

$$\hat{\boldsymbol{T}}_{ij} = \hat{\boldsymbol{T}} + \frac{\Delta \hat{\boldsymbol{T}} \boldsymbol{g}_{ij} \boldsymbol{e}_j^T \hat{\boldsymbol{T}}}{1 - \Delta \boldsymbol{e}_j^T \hat{\boldsymbol{T}} \boldsymbol{g}_{ij}}$$

and $\boldsymbol{g}_{ij}$ is computed using

$$\boldsymbol{g}_{ij} = \frac{\partial \left\{ \frac{\boldsymbol{t}_j}{\|\boldsymbol{t}_j\|} \right\}}{\partial t_{ij}} = \frac{1}{\|\boldsymbol{t}_j\|^3} (t_{ij} \boldsymbol{t}_j - \|\boldsymbol{t}_j\|^2 \boldsymbol{e}_i)$$

with

$$\{\boldsymbol{t}_1, \boldsymbol{t}_2, \ldots, \boldsymbol{t}_{m+n}\} = \{\boldsymbol{t}_{11}, \boldsymbol{t}_{12}, \ldots, \boldsymbol{t}_{1m}\} \cup \{\boldsymbol{t}_{41}, \boldsymbol{t}_{42}, \ldots, \boldsymbol{t}_{4n}\}.$$

2) Case 2: $\boldsymbol{D}$ Is a Block-Diagonal Matrix: Matrix $\boldsymbol{D}$ in this case assumes the form

$$\boldsymbol{D} = \boldsymbol{D}_1 \oplus \boldsymbol{D}_4 \tag{31}$$

where $\boldsymbol{D}_1$ and $\boldsymbol{D}_4$ are $m \times m$ and $n \times n$ matrices, respectively. The gradient of $J(\boldsymbol{x})$ can be derived as follows:

$$\begin{aligned}
\frac{\partial J(\boldsymbol{x})}{\partial t_{ij}} &= 2\beta_1 + 2(1-\mu)(\beta_2 - \beta_3) \\
\frac{\partial J(\boldsymbol{x})}{\partial d_{ij}} &= 2(1-\mu)\boldsymbol{e}_i^T \hat{\boldsymbol{T}} \hat{\boldsymbol{W}}_o (\hat{\boldsymbol{T}}^T \boldsymbol{D} - \hat{\boldsymbol{A}} \hat{\boldsymbol{T}}^T) \boldsymbol{e}_j
\end{aligned} \tag{32}$$

where

$$\begin{aligned}
\beta_1 &= \boldsymbol{e}_j^T \hat{\boldsymbol{T}} [(1-\mu)(\hat{\boldsymbol{A}}^T \hat{\boldsymbol{W}}_o \hat{\boldsymbol{A}} + \hat{\boldsymbol{C}}) + \mu \hat{\boldsymbol{W}}_o] \hat{\boldsymbol{T}}^T \hat{\boldsymbol{T}} \boldsymbol{g}_{ij} \\
\beta_2 &= \boldsymbol{e}_j^T \hat{\boldsymbol{T}} \hat{\boldsymbol{W}}_o \hat{\boldsymbol{T}}^T \boldsymbol{D} \boldsymbol{D}^T \hat{\boldsymbol{T}} \boldsymbol{g}_{ij} \\
\beta_3 &= \boldsymbol{e}_j^T \hat{\boldsymbol{T}} (\hat{\boldsymbol{A}}^T \hat{\boldsymbol{W}}_o \hat{\boldsymbol{T}}^T \boldsymbol{D} + \hat{\boldsymbol{W}}_o \hat{\boldsymbol{A}} \hat{\boldsymbol{T}}^T \boldsymbol{D}^T) \hat{\boldsymbol{T}} \boldsymbol{g}_{ij}
\end{aligned}$$

with $\boldsymbol{g}_{ij}$ defined in (30). In (32), $d_{ij} \in \boldsymbol{D}_1 \oplus \boldsymbol{D}_4$ is meant to be $d_{ij} \in \boldsymbol{D}_1$ for $(1,1) \le (i,j) \le (m,m)$ and $d_{ij} \in \boldsymbol{D}_4$ for $(m+1, m+1) \le (i,j) \le (m+n, m+n)$.

3) Case 3: $\boldsymbol{D}$ Is a Diagonal Matrix: Here, matrix $\boldsymbol{D}$ assumes the form

$$\boldsymbol{D} = \operatorname{diag}\{d_{11}, d_{22}, \ldots, d_{m+n,m+n}\}. \tag{33}$$

In this case, $\partial J(\boldsymbol{x}) / \partial d_{ij}$ can be obtained using (32) as

$$\frac{\partial J(\boldsymbol{x})}{\partial d_{ii}} = 2(1-\mu)\boldsymbol{e}_i^T \hat{\boldsymbol{T}} \hat{\boldsymbol{W}}_o (\hat{\boldsymbol{T}}^T \boldsymbol{D} - \hat{\boldsymbol{A}} \hat{\boldsymbol{T}}^T) \boldsymbol{e}_i \tag{34}$$

where $1 \le i \le m+n$, and $\partial J(\boldsymbol{x}) / \partial t_{ij}$ is also given by (32).

4) Case 4: $\boldsymbol{D}$ Is a Block-Scalar Matrix: It is assumed here that $\boldsymbol{D}_1 = \alpha \boldsymbol{I}_m$ and $\boldsymbol{D}_4 = \beta \boldsymbol{I}_n$ with scalars α and β. The gradient of $J(\boldsymbol{x})$ can then be calculated using

$$\begin{aligned}
\frac{\partial J(\boldsymbol{x})}{\partial \alpha} &= 2(1-\mu) \sum_{i=1}^{m} \boldsymbol{e}_i^T \hat{\boldsymbol{T}} \hat{\boldsymbol{W}}_o (\hat{\boldsymbol{T}}^T \boldsymbol{D} - \hat{\boldsymbol{A}} \hat{\boldsymbol{T}}^T) \boldsymbol{e}_i \\
\frac{\partial J(\boldsymbol{x})}{\partial \beta} &= 2(1-\mu) \sum_{i=1}^{n} \boldsymbol{e}_{m+i}^T \hat{\boldsymbol{T}} \hat{\boldsymbol{W}}_o (\hat{\boldsymbol{T}}^T \boldsymbol{D} - \hat{\boldsymbol{A}} \hat{\boldsymbol{T}}^T) \boldsymbol{e}_{m+i}
\end{aligned} \tag{35}$$

and $\partial J(\boldsymbol{x}) / \partial t_{ij}$ is computed using (32).

IV. Case Study

In this section, we present a case study to illustrate the effectiveness of the proposed algorithm. Consider a 2-D BIBO stable, separately locally controllable, and separately locally observable state-space digital filter $(\boldsymbol{A}^o, \boldsymbol{b}^o, \boldsymbol{c}^o, d)_{2,2}$ of order (2,2), where

$$\boldsymbol{A}^o = \begin{bmatrix} 1.88899 & -0.91219 & -1.00000 & 0.00000 \\ 1.00000 & 0.00000 & 0.00000 & 0.00000 \\ 0.02771 & -0.02580 & 1.88899 & 1.00000 \\ -0.02580 & 0.02431 & -0.91219 & 0.00000 \end{bmatrix}$$

$$\boldsymbol{b}^o = [0.219089 \quad 0.000000 \quad -0.028889 \quad 0.091219]^T$$

$$\boldsymbol{c}^o = [0.028889 \quad -0.091219 \quad -0.219089 \quad 0.000000]$$

$$d = 0.08900.$$

If a coordinate transformation matrix $\boldsymbol{T}^o = \boldsymbol{T}_1^o \oplus \boldsymbol{T}_4^o$ is chosen as

$$\boldsymbol{T}^o = \begin{bmatrix} -1.373341 & 9.544965 \\ -3.318699 & 9.494676 \end{bmatrix} \oplus \begin{bmatrix} 0.942406 & 0.329402 \\ -0.947397 & -0.136313 \end{bmatrix}$$

then the above filter is transformed to the *optimal realization* $(\boldsymbol{A}, \boldsymbol{b}, \boldsymbol{c}, d)_{2,2} = (\boldsymbol{T}^{o-1}\boldsymbol{A}^o\boldsymbol{T}^o, \boldsymbol{T}^{o-1}\boldsymbol{b}, \boldsymbol{c}\boldsymbol{T}^o, d)_{2,2}$ that satisfies (15) and (16) simultaneously [25], [26], where

$$\boldsymbol{A} = \begin{bmatrix} 0.923959 & -0.115198 & -0.480100 & -0.167811 \\ 0.178310 & 0.965031 & -0.167811 & -0.058655 \\ 0.045857 & 0.013210 & 0.923959 & 0.178310 \\ 0.013210 & 0.021491 & -0.115198 & 0.965031 \end{bmatrix}$$

$$\boldsymbol{b} = [0.111613 \quad 0.039012 \quad -0.142200 \quad 0.319129]^T$$

$$\boldsymbol{c} = [0.263054 \quad -0.590350 \quad -0.206471 \quad -0.072168]$$

$$d = 0.089000$$

and the local controllability and local observability Gramians were calculated by truncating the series in (12) and (9) to the range $(0,0) \le (i,j) \le (200,200)$ as

$$\boldsymbol{K}_c = \begin{bmatrix} 1.000000 & 0.221999 & 0.155751 & 0.036319 \\ 0.221999 & 1.000000 & 0.184141 & 0.064066 \\ 0.155751 & 0.184141 & 1.000000 & 0.221999 \\ 0.036319 & 0.064066 & 0.221999 & 1.000000 \end{bmatrix}$$

$$\boldsymbol{W}_o = \begin{bmatrix} 3.422064 & 0.759695 & 0.532989 & 0.630143 \\ 0.759695 & 3.422064 & 0.124286 & 0.219239 \\ 0.532989 & 0.124286 & 3.422064 & 0.759695 \\ 0.630143 & 0.219239 & 0.759695 & 3.422064 \end{bmatrix}$$

respectively. This gives the noise gain $I(\boldsymbol{0}) = \mathrm{tr}[\boldsymbol{W}_o] = 13.688256$. In what follows, EF and state-variable coordinate transformation are applied to the above *optimal realization* $(\boldsymbol{A}, \boldsymbol{b}, \boldsymbol{c}, d)_{2,2}$ in order to jointly minimize the roundoff noise, and the results obtained are then compared to their counterparts obtained in [29] where the minimization of the roundoff noise was carried out using EF and state-variable coordinate transformation, but in a *separate* manner.

1) Case 1: $\boldsymbol{D}$ Is a General Matrix: The quasi-Newton algorithm was applied to minimize (29) with $\mu = 0.01$ and tolerance $\varepsilon = 10^{-8}$. It took the algorithm ten iterations to converge to the solution

$$\hat{\boldsymbol{T}} = \begin{bmatrix} 1.112303 & -0.262415 \\ 0.768079 & 0.846247 \end{bmatrix} \oplus \begin{bmatrix} 0.977230 & -0.434117 \\ 0.059862 & 1.067639 \end{bmatrix}$$

or equivalently

$$\boldsymbol{T} = \begin{bmatrix} 1.076031 & 0.857797 \\ -0.136530 & 0.926745 \end{bmatrix} \oplus \begin{bmatrix} 0.922624 & 0.178741 \\ -0.322246 & 1.067644 \end{bmatrix}.$$

This leads to

$$\overline{\boldsymbol{A}} = \begin{bmatrix} 0.793657 & -0.235832 & -0.218781 & -0.149075 \\ 0.181787 & 1.095333 & -0.178900 & -0.121901 \\ 0.046747 & 0.047458 & 0.885610 & 0.190951 \\ 0.024675 & 0.043593 & -0.123522 & 1.003380 \end{bmatrix}$$

$$\overline{\boldsymbol{b}} = [0.062793 \quad 0.051347 \quad -0.200321 \quad 0.238447]^T$$

$$\overline{\boldsymbol{c}} = [0.363655 \quad -0.321457 \quad -0.167239 \quad -0.113955]$$

$$\overline{\boldsymbol{K}}_c = \begin{bmatrix} 1.000000 & -0.484097 & -0.009234 & -0.020689 \\ -0.484097 & 1.000000 & 0.190252 & 0.119536 \\ -0.009234 & 0.190252 & 1.000000 & 0.354179 \\ -0.020689 & 0.119536 & 0.354179 & 1.000000 \end{bmatrix}$$

$$\overline{\boldsymbol{W}}_o = \begin{bmatrix} 3.802789 & 3.394235 & 0.304627 & 0.791440 \\ 3.394235 & 6.664921 & 0.288432 & 0.896328 \\ 0.304627 & 0.288432 & 2.816605 & 0.091564 \\ 0.791440 & 0.896328 & 0.091564 & 4.299965 \end{bmatrix}.$$

Using (28) and (29), the optimal EF matrix $\boldsymbol{D}$ and the noise gain in (18) were found to be

$$\boldsymbol{D} = \begin{bmatrix} 0.793657 & -0.235832 & -0.218781 & -0.149075 \\ 0.181787 & 1.095333 & -0.178900 & -0.121901 \\ 0.046747 & 0.047458 & 0.885610 & 0.190951 \\ 0.024675 & 0.043593 & -0.123522 & 1.003380 \end{bmatrix}$$

and $I(\boldsymbol{D}, \boldsymbol{T}) = 0.276534$, respectively. The profile of $J(\hat{\boldsymbol{T}}^{-T}\hat{\boldsymbol{A}}\hat{\boldsymbol{T}}^T, \hat{\boldsymbol{T}})$ with $\mu = 0.01$ in (29) during the first 12 iterations of the algorithm is depicted in Fig. 1.

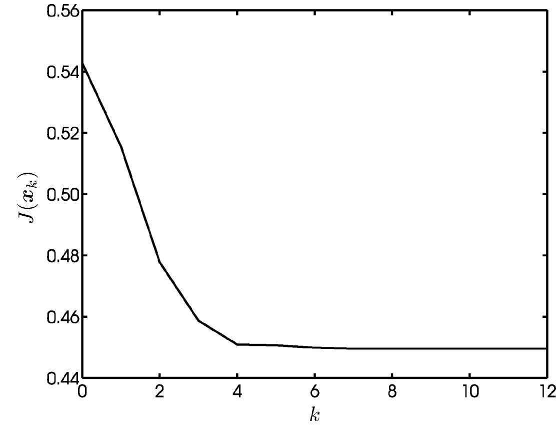

Fig. 1. Profile of $J(\hat{\boldsymbol{T}}^{-T}\hat{\boldsymbol{A}}\hat{\boldsymbol{T}}^T\hat{\boldsymbol{T}})$ with $\mu = 0.01$ during the first 12 iterations.

Next, the above optimal EF matrix $\boldsymbol{D}$ was rounded to a power-of-two representation with 3 bits after the binary point, which resulted in

$$\boldsymbol{D}_{3\mathrm{bit}} = \begin{bmatrix} 0.750 & -0.250 & -0.250 & -0.125 \\ 0.125 & 1.125 & -0.125 & -0.125 \\ 0.000 & 0.000 & 0.875 & 0.250 \\ 0.000 & 0.000 & -0.125 & 1.000 \end{bmatrix}.$$

The corresponding noise gain was found to be $I(\boldsymbol{D}_{3\mathrm{bit}}, \boldsymbol{T}) = 0.379031$. Furthermore, when the optimal EF matrix $\boldsymbol{D}$ was rounded to the integer representation $\boldsymbol{D}_{\mathrm{int}} = \mathrm{diag}\{1,1,1,1\}$, the noise gain was found to be $I(\boldsymbol{D}_{\mathrm{int}}, \boldsymbol{T}) = 1.786366$.

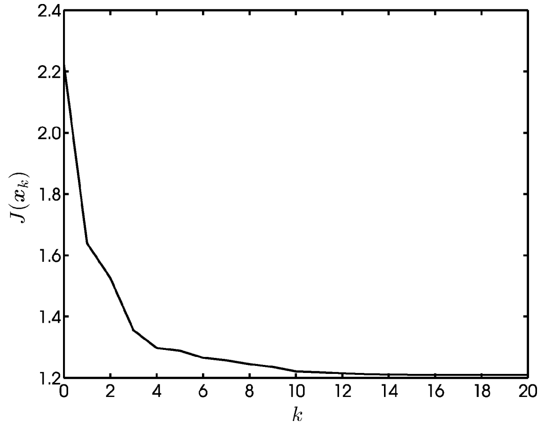

Fig. 2. Profile of $J(\boldsymbol{D}, \hat{T})$ with $\mu = 0.01$ during the first 20 iterations.

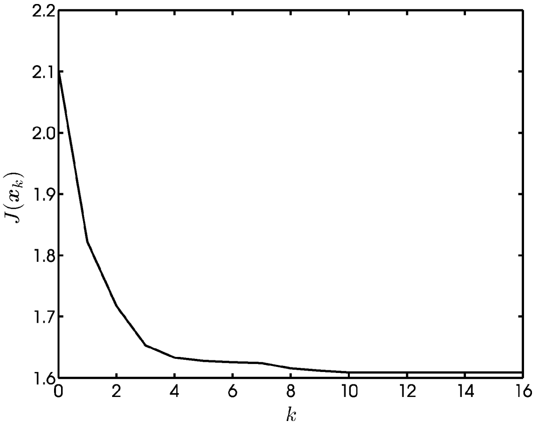

Fig. 3. Profile of $J(\boldsymbol{D}, \hat{\boldsymbol{T}})$ with $\mu = 0.0$ during the first 16 iterations.

2) Case 2: $\boldsymbol{D}$ Is a Block-Diagonal Matrix: Again, the quasi-Newton algorithm was applied to minimize $J(\boldsymbol{D}, \hat{\boldsymbol{T}})$ in (25) with $\boldsymbol{D} = \boldsymbol{D}_1 \oplus \boldsymbol{D}_4$, $\mu = 0.01$, and $\varepsilon = 10^{-8}$. It took the algorithm 19 iterations to converge to the solution

$$\hat{\boldsymbol{T}} = \begin{bmatrix} 1.075413 & -0.290485 \\ 0.734598 & 0.837413 \end{bmatrix} \oplus \begin{bmatrix} 1.081669 & -1.093278 \\ -0.110922 & 1.533936 \end{bmatrix}$$
$$\boldsymbol{D} = \begin{bmatrix} 0.812641 & -0.217981 \\ 0.174373 & 1.086382 \end{bmatrix} \oplus \begin{bmatrix} 0.720185 & 0.234829 \\ -0.263724 & 1.077042 \end{bmatrix}.$$

This leads to

$$\boldsymbol{T} = \begin{bmatrix} 1.036236 & 0.823539 \\ -0.168545 & 0.914226 \end{bmatrix} \oplus \begin{bmatrix} 0.952782 & 0.061110 \\ -0.965616 & 1.511947 \end{bmatrix}$$
$$\overline{\boldsymbol{A}} = \begin{bmatrix} 0.805454 & -0.228456 & -0.170347 & -0.163237 \\ 0.172688 & 1.083536 & -0.144340 & -0.138315 \\ 0.045256 & 0.049009 & 0.756447 & 0.269578 \\ 0.035561 & 0.051491 & -0.205808 & 1.132543 \end{bmatrix}$$
$$\overline{\boldsymbol{b}} = [0.064366 \quad 0.054539 \quad -0.156380 \quad 0.111198]^T$$
$$\overline{\boldsymbol{c}} = [\,0.372087 \quad -0.323078 \quad -0.127035 \quad -0.121732]$$
$$\overline{\boldsymbol{K}}_c = \begin{bmatrix} 1.000000 & -0.440602 & -0.007858 & -0.016928 \\ -0.440602 & 1.000000 & 0.198776 & 0.171103 \\ -0.007858 & 0.198776 & 1.000000 & 0.759746 \\ -0.016928 & 0.171103 & 0.759746 & 1.000000 \end{bmatrix}$$
$$\overline{\boldsymbol{W}}_o = \begin{bmatrix} 3.506411 & 3.007275 & -0.088578 & 0.963868 \\ 3.007275 & 6.325040 & -0.168173 & 1.121432 \\ -0.088578 & -0.168173 & 4.899437 & -3.747273 \\ 0.963868 & 1.121432 & -3.747273 & 7.975946 \end{bmatrix}$$

and the minimized noise gain was found to be $I(\boldsymbol{D}, \boldsymbol{T}) = 0.993119$ from (18). The profile of $J(\boldsymbol{D}, \hat{\boldsymbol{T}})$ with $\mu = 0.01$ in (25) during the first 20 iterations of the algorithm is shown in Fig. 2.

Next, the optimal EF matrix $\boldsymbol{D} = \boldsymbol{D}_1 \oplus \boldsymbol{D}_4$ was rounded to a power-of-two representation with 3 bits after the binary point to yield

$$\boldsymbol{D}_{3\text{bit}} = \begin{bmatrix} 0.875 & -0.250 \\ 0.125 & 1.125 \end{bmatrix} \oplus \begin{bmatrix} 0.750 & 0.250 \\ -0.250 & 1.125 \end{bmatrix}$$

which leads to a noise gain $I(\boldsymbol{D}_{3\text{bit}}, \boldsymbol{T}) = 1.026055$. Furthermore, the optimal EF matrix $\boldsymbol{D} = \boldsymbol{D}_1 \oplus \boldsymbol{D}_4$ was rounded to the integer representation $\boldsymbol{D}_{\text{int}} = \text{diag}\{1, 1, 1, 1\}$, and the corresponding noise gain was found to be $I(\boldsymbol{D}_{\text{int}}, \boldsymbol{T}) = 1.779801$.

3) Case 3: $\boldsymbol{D}$ Is a Diagonal Matrix: The quasi-Newton algorithm with $\mu = 0.0$ and $\varepsilon = 10^{-8}$ was applied to minimize (25) for a diagonal EF matrix $\boldsymbol{D}$. It took the algorithm 14 iterations to converge to the solution

$$\hat{\boldsymbol{T}} = \begin{bmatrix} 1.001398 & -0.305076 \\ 0.587614 & 0.866360 \end{bmatrix} \oplus \begin{bmatrix} 0.930738 & -0.766589 \\ 0.115699 & 1.200227 \end{bmatrix}$$
$$\boldsymbol{D} = \text{diag}\{0.959461,\ 0.979277,\ 0.896380,\ 0.950455\}$$

which leads to

$$\boldsymbol{T} = \begin{bmatrix} 0.961055 & 0.680708 \\ -0.191312 & 0.926574 \end{bmatrix} \oplus \begin{bmatrix} 0.839287 & 0.249038 \\ -0.657829 & 1.205640 \end{bmatrix}$$
$$\overline{\boldsymbol{A}} = \begin{bmatrix} 0.834922 & -0.203220 & -0.197375 & -0.217164 \\ 0.158082 & 1.054068 & -0.151112 & -0.166263 \\ 0.040783 & 0.038439 & 0.829877 & 0.216040 \\ 0.029372 & 0.044948 & -0.153937 & 1.059113 \end{bmatrix}$$
$$\overline{\boldsymbol{b}} = [0.075302 \quad 0.057652 \quad -0.213419 \quad 0.148249]^T$$
$$\overline{\boldsymbol{c}} = [0.365751 \quad -0.367940 \quad -0.125814 \quad -0.138428]$$
$$\overline{\boldsymbol{K}}_c = \begin{bmatrix} 1.000000 & -0.295774 & 0.021123 & 0.003433 \\ -0.295774 & 1.000000 & 0.193509 & 0.161263 \\ 0.021123 & 0.193509 & 1.000000 & 0.558757 \\ 0.003433 & 0.161263 & 0.558757 & 1.000000 \end{bmatrix}$$
$$\overline{\boldsymbol{W}}_o = \begin{bmatrix} 3.006599 & 2.209658 & 0.039163 & 0.801213 \\ 2.209658 & 5.481950 & -0.014649 & 0.881098 \\ 0.039163 & -0.014649 & 3.052508 & -1.354534 \\ 0.801213 & 0.881098 & -1.354534 & 5.642635 \end{bmatrix}$$

and the minimized noise gain was found to be $I(\boldsymbol{D}, \boldsymbol{T}) = 1.608812$ from (18). The profile of $J(\boldsymbol{D}, \hat{\boldsymbol{T}})$ with $\mu = 0.0$ in (25) during the first 16 iterations of the algorithm is shown in Fig. 3.

Next, the above optimal diagonal EF matrix $\boldsymbol{D}$ was rounded to a power-of-two representation with 3 bits after the binary point to yield $\boldsymbol{D}_{3\text{bit}} = \text{diag}\{1.000,\ 1.000,\ 0.875,\ 1.000\}$, which leads to a noise gain $I(\boldsymbol{D}_{3\text{bit}}, \boldsymbol{T}) = 1.631354$. Furthermore, when the optimized diagonal EF matrix $\boldsymbol{D}$ was rounded to the integer representation $\boldsymbol{D}_{\text{int}} = \text{diag}\{1, 1, 1, 1\}$, the noise gain was found to be $I(\boldsymbol{D}_{\text{int}}, \boldsymbol{T}) = 1.662735$.

TABLE I
PERFORMANCE COMPARISON

Matrix $\boldsymbol{D}$	Optimization	Accuracy of $\boldsymbol{D}$		
		Infinite Precision	3-Bit Quantization	Integer Quantization
Null	Separate	13.688256		
General	Separate	0.465549	0.555529	2.040208
	Joint	0.276534	0.379031	1.786366
Block-Diagonal	Separate	1.555329	1.612408	2.040208
	Joint	0.993119	1.026055	1.779801
Diagonal	Separate	1.908903	1.937559	2.040208
	Joint	1.608812	1.631354	1.662735
Block-Scalar	Separate	1.950396	1.965326	2.040208
	Joint	1.614538	1.650103	1.661235

4) Case 4: $\boldsymbol{D}$ Is a Block-Scalar Matrix: In this case, the quasi-Newton algorithm with $\mu = 0.0$ and $\varepsilon = 10^{-8}$ was applied to minimize (25) for $\boldsymbol{D} = \alpha\boldsymbol{I}_2 \oplus \beta\boldsymbol{I}_2$ with scalars α and β. The algorithm converges after 12 iterations to the solution

$$\hat{\boldsymbol{T}} = \begin{bmatrix} 1.009533 & -0.279518 \\ 0.567440 & 0.880511 \end{bmatrix} \oplus \begin{bmatrix} 0.917919 & -0.788744 \\ 0.134695 & 1.202726 \end{bmatrix}$$
$$\alpha = 0.972437, \quad \beta = 0.932446$$

which leads to

$$\boldsymbol{T} = \begin{bmatrix} 0.971994 & 0.662241 \\ -0.165006 & 0.938383 \end{bmatrix} \oplus \begin{bmatrix} 0.824073 & 0.268195 \\ -0.681278 & 1.210245 \end{bmatrix}$$
$$\overline{\boldsymbol{A}} = \begin{bmatrix} 0.833441 & -0.200869 & -0.194700 & -0.229679 \\ 0.161558 & 1.055549 & -0.139020 & -0.163997 \\ 0.041366 & 0.037287 & 0.827306 & 0.217046 \\ 0.030965 & 0.044882 & -0.155969 & 1.061684 \end{bmatrix}$$
$$\overline{\boldsymbol{b}} = [0.077249 \quad 0.055157 \quad -0.218369 \quad 0.140763]^T$$
$$\overline{\boldsymbol{c}} = [0.353098 \quad -0.379770 \quad -0.120980 \quad -0.142716]$$
$$\overline{\boldsymbol{K}}_c = \begin{bmatrix} 1.000000 & -0.297762 & 0.026165 & 0.007977 \\ -0.297762 & 1.000000 & 0.190338 & 0.162372 \\ 0.026165 & 0.190338 & 1.000000 & 0.563261 \\ 0.007977 & 0.162372 & 0.563261 & 1.000000 \end{bmatrix}$$
$$\overline{\boldsymbol{W}}_o = \begin{bmatrix} 3.082557 & 2.282800 & 0.017388 & 0.830929 \\ 2.282800 & 5.458336 & -0.037480 & 0.879969 \\ 0.017388 & -0.037480 & 3.059210 & -1.446363 \\ 0.830929 & 0.879969 & -1.446363 & 5.751581 \end{bmatrix}$$

and the minimized noise gain was found to be $I(\boldsymbol{D}, \boldsymbol{T}) = 1.614538$ from (18). The profile of $J(\boldsymbol{D}, \hat{\boldsymbol{T}})$ with $\mu = 0.0$ in (25) during the first 14 iterations of the algorithm is drawn in Fig. 4.

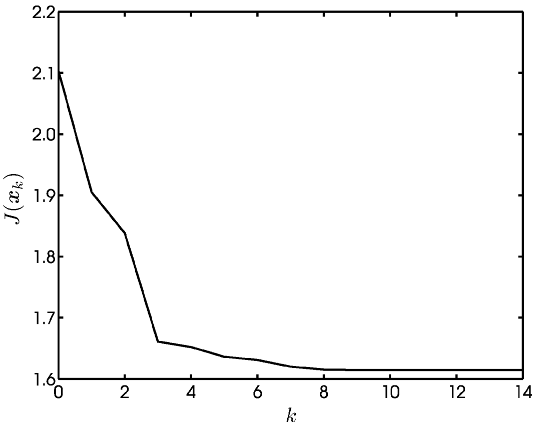

Fig. 4. Profile of $J(\boldsymbol{D}, \hat{\boldsymbol{T}})$ with $\mu = 0.0$ during the first 14 iterations.

Next, the optimal EF matrix $\boldsymbol{D} = \alpha\boldsymbol{I}_2 \oplus \beta\boldsymbol{I}_2$ was rounded to a power-of-two representation with 3 bits after the binary point as well as an integer representation. It was found that these representations were given by $\boldsymbol{D}_{3\text{bit}} = \text{diag}\{1.000, 1.000, 0.875, 0.875\}$ and $\boldsymbol{D}_{\text{int}} = \text{diag}\{1, 1, 1, 1\}$, respectively. The corresponding noise gains were obtained as $I(\boldsymbol{D}_{3\text{bit}}, \boldsymbol{T}) = 1.650103$ and $I(\boldsymbol{D}_{\text{int}}, \boldsymbol{T}) = 1.661235$, respectively. It is interesting to note that for this particular example the noise gain obtained from the integer approximation of the optimal matrix $\boldsymbol{D} = \alpha\boldsymbol{I}_m \oplus \beta\boldsymbol{I}_n$ is smaller than that obtained from the integer approximation of the optimal diagonal EF matrix $\boldsymbol{D}$, due to their different $\hat{\boldsymbol{T}}$ matrices.

The simulation results described above are summarized using the noise gain $I(\boldsymbol{D}, f\boldsymbol{T})$ in (18) in Table I. For comparison purposes, their counterparts obtained using the method in [29] are also included in the table. Specifically, the term "separate" means that the EF matrix was optimized by applying the existing method [29] to the optimal realization without EF, which satisfies (15) and (16) simultaneously [25], [26]. From the Table, it is observed that the proposed joint optimization offers greatly reduced roundoff noise gain for all cases of the matrix $\boldsymbol{D}$ when compared with that obtained by using *separate* optimization.

V. CONCLUSION

The joint optimization problem of EF and realization to minimize the effects of roundoff noise of 2-D state-space digital filters subject to L_2-norm dynamic-range scaling constraints has been investigated. It has been shown that the problem at hand can be converted into an unconstrained optimization problem by using linear algebraic techniques. Closed-form formulas for fast evaluation of the gradient of the objective function have been derived and an efficient quasi-Newton algorithm has been employed to solve the unconstrained optimization problem. The proposed technique has been applied to the cases where the EF matrix is a general, block-diagonal, diagonal, or block-scalar matrix, and its effectiveness compared with the existing method [29] has been demonstrated by a case study.

References

[1] H. A. Spang, III and P. M. Shultheiss, "Reduction of quantizing noise by use of feedback," *IRE Trans. Commun. Syst.*, vol. CS-10, pp. 373–380, Dec. 1962.

[2] T. Thong and B. Liu, "Error spectrum shaping in narrowband recursive digital filters," *IEEE Trans. Acoust. Speech, Signal Process.*, vol. ASSP-25, pp. 200–203, Apr. 1977.

[3] T. L. Chang and S. A. White, "An error cancellation digital filter structure and its distributed-arithmetic implementation," *IEEE Trans. Circuits Syst.*, vol. CAS-28, pp. 339–342, Apr. 1981.

[4] D. C. Munson and D. Liu, "Narrowband recursive filters with error spectrum shaping," *IEEE Trans. Circuits Syst.*, vol. CAS-28, pp. 160–163, Feb. 1981.

[5] W. E. Higgins and D. C. Munson, "Noise reduction strategies for digital filters: Error spectrum shaping versus the optimal linear state-space formulation," *IEEE Trans. Acoust. Speech, Signal Process.*, vol. ASSP-30, pp. 963–973, Dec. 1982.

[6] M. Renfors, "Roundoff noise in error-feedback state-space filters," in *Proc. Int. Conf. Acoust., Speech, Signal Process. (ICASSP'83)*, Apr. 1983, pp. 619–622.

[7] W. E. Higgins and D. C. Munson, "Optimal and suboptimal error-spectrum shaping for cascade-form digital filters," *IEEE Trans. Circuits Syst.*, vol. CAS-31, pp. 429–437, May 1984.

[8] T. I. Laakso and I. O. Hartimo, "Noise reduction in recursive digital filters using high-order error feedback," *IEEE Trans. Signal Process.*, vol. 40, pp. 1096–1107, May 1992.

[9] P. P. Vaidyanathan, "On error-spectrum shaping in state-space digital filters," *IEEE Trans. Circuits Syst.*, vol. 32, pp. 88–92, Jan. 1985.

[10] D. Williamson, "Roundoff noise minimization and pole-zero sensitivity in fixed-point digital filters using residue feedback," *IEEE Trans. Acoust., Speech, Signal Process.*, vol. ASSP-34, pp. 1210–1220, Oct. 1986.

[11] T. Hinamoto, S. Karino, and N. Kuroda, "Error spectrum shaping in 2-D digital filters," in *Proc. IEEE Int. Symp. Circuits Syst. (ISCAS'95)*, May 1995, vol. 1, pp. 348–351.

[12] P. Agathoklis and C. Xiao, "Low roundoff noise structures for 2-D filters," in *Proc. IEEE Int. Symp. Circuits Syst. (ISCAS'96)*, May 1996, vol. 2, pp. 352–355.

[13] T. Hinamoto, S. Karino, and N. Kuroda, "2-D state-space digital filters with error spectrum shaping," in *Proc. IEEE Int. Symp. Circuits Syst. (ISCAS'96)*, May 1996, vol. 2, pp. 766–769.

[14] T. Hinamoto, N. Kuroda, and T. Kuma, "Error feedback for noise reduction in 2-D digital filers with quadrantally symmetric or antisymmetric coefficients," in *Proc. IEEE Int. Symp. Circuits Syst. (ISCAS'97)*, Jun. 1997, vol. 4, pp. 2461–2464.

[15] T. Hinamoto, S. Karino, N. Kuroda, and T. Kuma, "Error spectrum shaping in two-dimensional recursive digital filters," *IEEE Trans. Circuits Syst.*, vol. 46, pp. 1203–1215, Oct. 1999.

[16] G. Li and M. Gevers, "Roundoff noise minimization using delta-operator realizations," *IEEE Trans. Signal Process.*, vol. 41, pp. 629–637, Feb. 1993.

[17] D. Williamson, "Delay replacement in direct form structures," *IEEE Trans. Acoust., Speech, Signal Process.*, vol. 36, pp. 453–460, Apr. 1988.

[18] M. M. Ekanayake and K. Premaratne, "Two-dimensional delta-operator formulated discrete-time systems: Analysis and synthesis of minimum roundoff noise realizations," in *Proc. IEEE Int. Symp. Circuits Syst. (ISCAS'96)*, May 1996, vol. 2, pp. 213–216.

[19] G. Li and Z. Zhao, "On the generalized DFIIt structure and its state-space realization in digital filter implementation," *IEEE Trans. Circuits Syst. I*, vol. 51, pp. 769–778, Apr. 2004.

[20] S. Y. Hwang, "Roundoff noise in state-space digital filtering: A general analysis," *IEEE Trans. Acoust., Speech, Signal Process.*, vol. ASSP-24, pp. 256–262, Jun. 1976.

[21] C. T. Mullis and R. A. Roberts, "Synthesis of minimum roundoff noise fixed-point digital filters," *IEEE Trans. Circuits Syst.*, vol. CAS-23, pp. 551–562, Sep. 1976.

[22] S. Y. Hwang, "Minimum uncorrelated unit noise in state-space digital filtering," *IEEE Trans. Acoust., Speech, Signal Process.*, vol. ASSP-25, pp. 273–281, Aug. 1977.

[23] L. B. Jackson, A. G. Lindgren, and Y. Kim, "Optimal synthesis of second-order state-space structures for digital filters," *IEEE Trans. Circuits Syst.*, vol. CAS-26, pp. 149–153, Mar. 1979.

[24] M. Kawamata and T. Higuchi, "Synthesis of 2-D separable denominator digital filters with minimum roundoff noise and no overflow oscillations," *IEEE Trans. Circuits Syst.*, vol. CAS-33, pp. 365–372, Apr. 1986.

[25] ——, "A unified study on the roundoff noise in 2-D state-space digital filters," *IEEE Trans. Circuits Syst.*, vol. CAS-33, pp. 724–730, Jul. 1986.

[26] W.-S. Lu and A. Antoniou, "Synthesis of 2-D state-space fixed-point digital filter structures with minimum roundoff noise," *IEEE Trans. Circuits Syst.*, vol. CAS-33, pp. 965–973, Oct. 1986.

[27] T. Hinamoto, T. Hamanaka, and S. Maekawa, "A generalized study on the synthesis of 2-D state-space digital filters with minimum roundoff noise," *IEEE Trans. Circuits Syst.*, vol. 35, pp. 1037–1042, Aug. 1988.

[28] T. Hinamoto, H. Ohnishi, and W.-S. Lu, "Roundoff noise minimization of state-space digital filters using separate and joint error feedback/coordinate transformation," *IEEE Trans. Circuits Syst. I*, vol. 50, pp. 23–33, Jan. 2003.

[29] T. Hinamoto, K. Higashi, and W.-S. Lu, "Separate/joint optimization of error feedback and coordinate transformation for roundoff noise minimization in two-dimensional state-space digital filters," *IEEE Trans. Signal Process.*, vol. 51, pp. 2436–2445, Sep. 2003.

[30] W.-S. Lu and T. Hinamoto, "Jointly optimized error-feedback and realization for roundoff noise minimization in state-space digital filters," *IEEE Trans. Signal Processing*, vol. 53, pp. 2135–2145, Jun. 2005.

[31] R. Fletcher, *Practical Methods of Optimization*, 2nd ed. New York: Wiley, 1987.

[32] R. P. Roesser, "A discrete state-space model for linear image processing," *IEEE Trans. Autom. Control*, vol. 20, pp. 1–10, Feb. 1975.

[33] S. Kung, B. C. Levy, M. Morf, and T. Kailath, "New results in 2-D systems theory, Part II: 2-D state-space models—Realization and notions of controllability, observability, and minimality," *Proc. IEEE*, vol. 65, pp. 945–961, Jun. 1977.

[34] T. Kailath, *Linear Systems*. Englewood Cliffs, NJ: Prentice-Hall, 1980.

Takao Hinamoto (M'77–SM'84–F'01) received the B.E. degree from Okayama University, Okayama, Japan, in 1969, the M.E. degree from Kobe University, Kobe, Japan, in 1971, and the Dr.Eng. degree from Osaka University, Osaka, Japan, in 1977, all in electrical engineering.

From 1972 to 1988, he was with the Faculty of Engineering, Kobe University. From 1979 to 1981, he was a Visiting Member of Staff in the Department of Electrical Engineering, Queen's University, Kingston, ON, Canada, on leave from Kobe University. During 1988–1991, he was a Professor of electronic circuits in the Faculty of Engineering, Tottori University, Tottori, Japan. Since 1992, he has been a Professor of Electronic Control in the Department of Electrical Engineering, Hiroshima University, Hiroshima, Japan. His research interests include digital signal processing, system theory, and control engineering. He has published about 350 papers in these areas and is the Coeditor of *Two-Dimensional Signal and Image Processing* (Tokyo, Japan: SICE, 1996). He was Guest Editor of the special sections on Digital Signal Processing and on Adaptive Signal Processing and Its Applications in the *IEICE Transactions on Fundamentals* in August 1998 and March 2005, respectively. He was the Co-Guest Editor of the special section on Recent Advances in Circuits and Systems in the July and August 2005 issues of *IEICE Transactions on Information and Systems*. He was Chair of the 12th Digital Signal Processing (DSP) Symposium in Hiroshima, Japan, in November 1997, sponsored by the DSP Technical Committee of IEICE. He was a member of the Technical Program Committee for ISCAS'99 and an International Coordinator of the Organizing Committee for ISCAS'04. From 1993 to 2000, he was a Senator or Member of the Board of Directors in the Society of Instrument and Control Engineers (SICE), and from 1999 to 2001 he was Chair of the Chugoku Chapter of SICE. From June 2003 to May 2004, he was Chair of the DSP Technical Committee of IEICE and Chair of the Chugoku Chapter of IEICE.

Dr. Hinamoto is a Fellow of IEICE and SICE. He received the IEEE Third Millennium Medal. He was an Associate Editor of the IEEE TRANSACTIONS ON CIRCUITS AND SYSTEMS—II: ANALOG AND DIGITAL SIGNAL PROCESSING from 1993 to 1995 and of the IEEE TRANSACTIONS ON CIRCUITS AND SYSTEMS—I: FUNDAMENTAL THEORY AND APPLICATIONS from 2002 to 2003 and since January 2006. He also served as the General Chair of the 47th IEEE International Midwest Symposium on Circuits and Systems held in Hiroshima, Japan, in July 2004. Since 1995, he has been a member of the Steering Committee of the IEEE International Midwest Symposium on Circuits and Systems and, since 1998, a member of the Digital Signal Processing Technical Committee of the IEEE Circuits and Systems Society. He played a leading role in establishing the Hiroshima Section of IEEE and was Interim Chair of the Section.

Hiroaki Ohnishi received the B.E. and M.E. degrees in electrical engineering from Hiroshima University, Hiroshima, Japan, in 2001 and 2003, respectively.

He was engaged in research on digital signal processing during his graduate studies. Since April 2003, he has been with Sanyo Electric Corporation, Osaka, Japan.

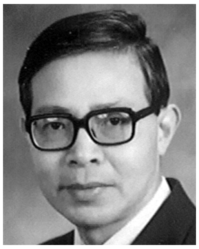

Wu-Sheng Lu (F'99) received the B.Sc. degree in mathematics from Fudan University, Shanghai, China, in 1964. He received the M.S. degree in electrical engineering and the Ph.D. degree in control science from the University of Minnesota, Minneapolis, in 1983 and 1984, respectively.

He was a Postdoctoral Fellow at the University of Victoria, Victoria, B.C., Canada, in 1985 and a Visiting Assistant Professor with the University of Minnesota in 1986. Since 1987, he has been with the University of Victoria, where he is a Professor. His current teaching and research interests are in the general areas of digital signal processing and application of optimization methods. He is coauthor (with A. Antoniou) of *Two-Dimensional Digital Filters* (Berlin, Germany: Marcel Dekker, 1992). Presently, he is Associate Editor of the *International Journal of Multidimensional Systems and Signal Processing.* He was an Associate Editor of the *Canadian Journal of Electrical and Computer Engineering* in 1989 and Editor from 1990 to 1992.

Dr. Lu is a Fellow of the Engineering Institute of Canada. He was an Associate Editor of the IEEE TRANSACTIONS ON CIRCUITS AND SYSTEMS—II: ANALOG AND DIGITAL SIGNAL PROCESSING from 1993 to 1995 and of the IEEE TRANSACTIONS ON CIRCUITS AND SYSTEMS—I: FUNDAMENTAL THEORY AND APPLICATIONS from 1999 to 2001 and from 2004 to 2005.